On Spatial Capacity of Wireless Ad Hoc Networks with Threshold Based Scheduling

Yue Ling Che, Rui Zhang, Yi Gong, and Lingjie Duan

arXiv:1409.2592v1 [cs.IT] 9 Sep 2014

Abstract

This paper studies spatial capacity in a stochastic wireless *ad hoc* network, where multi-stage probing and data transmission are sequentially performed. We propose a novel signal-to-interference-ratio (SIR) threshold based scheduling scheme: by starting with initial probing, each transmitter iteratively decides to further probe or stay idle, depending on whether the estimated SIR in the proceeding probing is larger or smaller than a predefined threshold. Since only local SIR information is required for making transmission decision, the proposed scheme is appropriate for distributed implementation in practical wireless ad hoc networks. Although one can assume that the transmitters are initially deployed according to a homogeneous Poisson point process (PPP), the SIR based scheduling makes the PPP no longer applicable to model the locations of retained transmitters in the subsequent probing and data transmission phases, due to the interference induced coupling in their decisions. As the analysis becomes very complicated, we first focus on single-stage probing and find that when the SIR threshold is set sufficiently small to assure an acceptable interference level in the network, the proposed scheme can greatly outperform the non-scheduling reference scheme in terms of spatial capacity. We clearly characterize the spatial capacity and obtain exact/approximate closed-form expressions, by proposing a new approximate approach to deal with the correlated SIR distributions over non-Poisson point processes. Then we successfully extend to multi-stage probing by properly designing the multiple SIR thresholds to assure gradual improvement of the spatial capacity. Furthermore, we analyze the impact of multi-stage probing overhead and present a probing-capacity tradeoff in scheduling design. Finally, extensive numerical results are presented to demonstrate the performance of the proposed scheduling as compared to existing schemes.

Index Terms

Wireless ad hoc network, threshold based scheduling, spatial capacity, stochastic geometry.

I. Introduction

Wireless *ad hoc* networks have emerged as a promising technology that can provide seamless communication between wireless users (transmitter-receiver pairs) without relying on any pre-existing infrastructure. In such

This work has been presented in part at *IEEE International Symposium on Information Theory (ISIT), Istanbul, Turkey, July 7-12, 2013.*

Y. L. Che and Y. Gong are with the School of Electrical and Electronic Engineering, Nanyang Technological University, Singapore (e-mail: chey0004@ntu.edu.sg; eygong@ntu.edu.sg).

R. Zhang is with the Department of Electrical and Computer Engineering, National University of Singapore (e-mail: elezhang@nus.edu.sg). He is also with the Institute for Infocomm Research, A*STAR, Singapore.

L. Duan is with the Engineering Systems and Design Pillar, Singapore University of Technology and Design (e-mail: lingjie_duan@sutd.edu.sg).

networks, the wireless users communicate with each other in a distributed manner. Due to the lack of centralized coordinators to coordinate the transmissions among the users, the wireless ad hoc network is under competitive and interference-dominant environment in nature. Thereby, efficient transmission schemes for transmitters to effectively schedule/adapt their transmissions are appealing for system performance improvement, and thus have attracted wide research attentions in the past decade.

Traditionally, each transmitter is enabled to independently decide whether to transmit over a particular channel based on its own willingness or channel strength [1]-[4], and the transmission rate of each user can be maximized by finding an optimal transmission probability or an optimal channel strength threshold, respectively. Although easy to be implemented, such independent transmission schemes do not consider the resulting user interactions in the wireless ad hoc networks due to the co-channel interference, and thus do not achieve high system performance in general cases. Therefore, more complex transmission schemes have been proposed to exploit the user interactions by exploring the information of signal-to-interference-ratio (SIR). For example, by iteratively adapting the transmit power level based on the estimated SIR, the Foschini-Miljanic algorithm [5] assures zero outage probability and/or minimum aggregate power consumption for uplink transmission in a cellular network. In [6], Yates has studied power convergence conditions for such iterative power control algorithms. Moreover, there have been some recent studies (e.g. [7] and [8]) that extend the Foschini-Miljanic algorithm to the wireless ad hoc network through joint scheduling and power control transmission schemes. In addition, by adapting the transmission probability depending on the received SIR, [9] has studied various random access schemes to improve the system throughput and/or the user fairness. However, [5]-[9] either require each transmitter to know at least the wireless environment information of its neighbors, or are of high implementation complexity, and thus are not appropriate for practical large-scale wireless ad hoc networks.

On the other hand, due to the randomized location of each transmitter and the effects of channel fading, the network-level performance analysis is fundamentally important for the study of wireless ad hoc networks. It is noted that Gupta and Kumar in [10] studied *scaling laws*, which quantified the increase of the volume of capacity region over the number of transmitters in ad hoc networks. Moreover, to determine the set of active transmitters that can yield maximum aggregate Shannon capacity in the network, the authors in [11]-[13] addressed the capacity maximization problem for an arbitrary wireless ad hoc network. However, [10]-[13] did not consider the impact of *spatial configuration* of the ad hoc network, which is a critical factor that determines the ad hoc network capacity [14]. It came to our attention that as a powerful tool to capture the impact of wireless users' spatial randomness on the network performance, stochastic geometry [15] is able to provide more comprehensive

characterization of the performance of wireless networks, and thus has attracted great attentions from both academy and industry [14], [16]. Among all the tools provided by stochastic geometry, homogeneous Poisson point process (PPP) [17] is the most widely used one for network topology modeling and performance analysis. Under the assumption that the transmitters are deployed according to a homogeneous PPP, the exact/approximate capacity of a wireless ad hoc network under various *independent* transmission schemes, such as Aloha-based random transmission [1], channel-inversion based power control [2], and channel-threshold based scheduling [3], [4], can all be successfully characterized by using advanced tools from stochastic geometry. However, limited work based on stochastic geometry has studied SIR-based transmission schemes, where the *user interactions* are involved. It is noted that [18] studied a probability-based scheduling scheme, where each transmitter independently adjusts its current transmission probability based on the received SIR in the proceeding iteration. However, [18] only studied the convergence of the probability-based scheduling, without addressing the network capacity with spatiality distributed users. To our best knowledge, there has been no existing work on studying the wireless ad hoc network capacity with a SIR-based transmission scheme. Hence, the impact of SIR-based transmissions is limitedly understood from the network-level point of view.

A principle goal of this study is to use stochastic geometry to fill the void of wireless network capacity characterization by an efficient SIR-based transmission scheme. To this end, we propose a novel SIR-threshold based scheduling scheme for a single-hop slotted wireless ad hoc network. We consider a probe-and-transmit protocol, where multi-stage probings are sequentially performed to gradually determine the transmitters that are allowed to transmit data in each slot. Specifically, we assume there are in total N probing phases and one data transmission phase in each slot, $1 \leq N < \infty$. We sequentially label the N probing phases as P-Phase 0, P-Phase 1, ..., and P-Phase $N-1$, and label the data transmission phase as D-Phase. As illustrated in Fig. 1, if the feedback SIR from receiver i in P-Phase $k-1$, $1 \leq k \leq N-1$, is no smaller than a pre-defined threshold, transmitter i decides to transmit in P-Phase k; otherwise, to improve the system throughput as well as save its own energy, transmitter i stays idle in the remaining time of the slot as in [19], so as to let other transmitters that have higher SIR levels re-contend the current transmission opportunity. Since each transmitter only requires direct-channel SIR feedback from its intended receiver for limited times, the proposed scheme is appropriate for distributed implementation in practical wireless ad hoc networks. In this paper, we characterize the wireless ad hoc network capacity with a metric called *spatial capacity*, which has been used in [20] and gives the average number of successful transmitters per unit area for any given initial transmitter density. We aim at closed-form spatial capacity characterization and maximization by exploring the SIR-threshold based transmission.

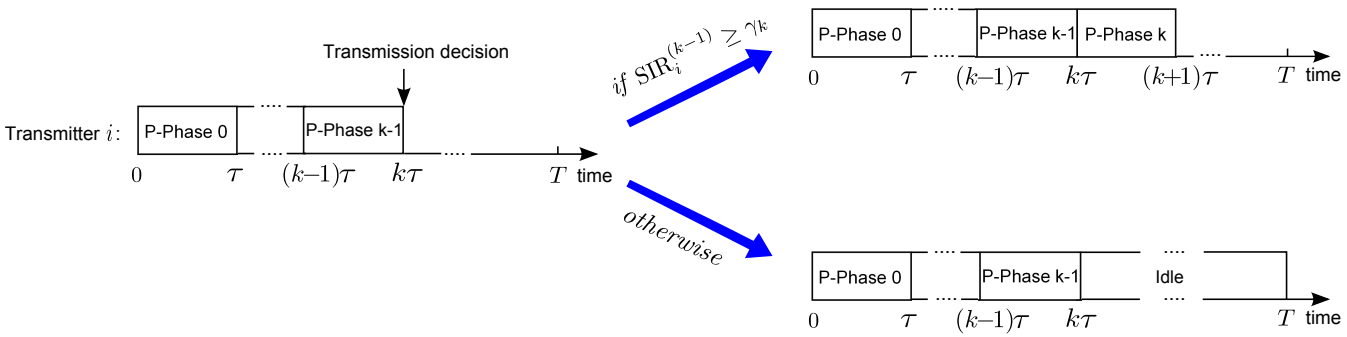

Fig. 1. Illustration of the SIR-threshold based transmission in P-Phase k: If the SIR in P-Phase $k-1$ is no smaller than the threshold $\gamma_k \geq 0$ in P-Phase k, the transmitter decides to transmit in P-Phase k; otherwise, it stays idle in the remaining time of this slot.

The key contributions of this paper are summarized as follows.

- *Novel SIR-threshold based scheduling scheme:* In Section II, we propose a novel SIR-threshold based transmission scheme for a single-hop wireless ad hoc network, which can be implemented efficiently in a distributed manner. Though one can use a homogeneous PPP to model the stochastic locations of the transmitters in the initial probing phase, we find that due to the iterative SIR-based scheduling, the PPP model is no longer applicable to model the locations of the retained transmitters in all the subsequent probing or data transmission phases. Furthermore, since the SIR distributions in all the probing and data transmission phases are strongly correlated, it is challenging to analyze/characterize the spatial capacity of the proposed scheme.
- *Single-stage probing for spacial capacity improvement:* In Section III, we start up with single-stage probing ($N = 1$) to clearly decide the SIR threshold for the proposed scheme and characterize the spatial capacity. We show that a small SIR threshold can efficiently reduce the retained transmitter number and thus the interference level in the data transmission phase, while a large SIR threshold will overly reduce the retained transmitter number and does not help improve the spatial capacity. We also propose a new approximate approach to characterize the spatial capacity in closed-form, which is useful for analyzing performance of wireless networks with interacted transmitters.
- *Multi-stage probing for spatial capacity improvement:* In Section IV, we extend proposed scheduling scheme from the single-stage probing ($N = 1$) to multi-stage probing ($N > 1$) for greater spatial capacity improvement. We show that once a sequence of increasing SIR thresholds are properly decided over probing phases, the spatial capacity is assured to gradually improve. As multi-stage probing can introduce non-ignorable overhead in each time slot, which reduces the spatial capacity, we study an interesting probing-capacity tradeoff over the probing-stage number N.
- *Performance evaluations for network design:* In both Section III and Section IV, we also provide extensive

numerical results to further evaluate the impact of key parameters of the proposed scheme. In particular, we present a density-capacity tradeoff in Section III-C-1), which shows that a small initial transmitter density can help improve the spatial capacity, while a large one will introduce high interference level and thus reduce the spatial capacity. To highlight the spatial capacity improvement performance of the proposed scheme, we also compare the proposed scheme with existing distributed scheduling schemes in Section III-C-2). Moreover, we consider a practical scenario with SIR estimation and feedback errors and show that the proposed design is robust to the SIR errors in Section III-C-3) by simulation. In Section IV, we study an example with $N = 2$ and show the corresponding spatial capacity over both SIR thresholds in P-Phase 1 and D-Phase. Interestingly, our numerical results show that the former SIR threshold plays a more critical role in determining the spatial capacity than the latter one, since the former SIR threshold decides how many transmitters can have a second chance to contend the transmission opportunity.

It is noted that some of the existing work has addressed the throughput/capacity analysis of a wireless communication system from the information-theoretic point of view. For example, Tse and Hanly considered a multipoint-to-point system and characterized the throughput capacity region and delay-limited capacity region of the fading multiple-access channel in [21] and [22], respectively, where the optimal power and/or rate allocation that can achieve the boundary of the capacity regions was derived. Although appealing, both [21] and [22] have assumed multiuser detection at a centralized receiver and ignored the impact of the random network topology driven by mobile transmitters and receivers mobility, and thus cannot completely provide network-level system performance characterization with distributed single-user detection (i.e., treating the multiuser interference as noise) receivers. Unlike Tse and Hanly's works in [21] and [22], we use stochastic geometry to model the large-scale random wireless ad hoc network topology, and novelly analyze the network-level performance of the iterative SIR-threshold based scheduling.

In addition, it is also noted that some existing work has adopted tools from stochastic geometry to study the non-PPP based wireless network. For example, by using a PPP to approximate the underlying non-PPP based spatial distribution of the transmitters' locations, [23]-[27] have successfully characterized the non-PPP based wireless network capacity. Unlike [23]-[27], due to the iterative SIR-based scheduling of the proposed scheme, we need to address not only the non-PPP based spatial distribution of the transmitters' locations, but also the resulting strongly-correlated SIR distributions over all probing and data transmission phases. To our best knowledge, such correlated SIR analysis/chracterization in non-PPP based wireless networks has not been addressed in the existing work based on stochastic geometry.

II. System Model and Performance Metric

In this section, we describe the considered transmission schemes in this paper. We then develop the network model based on stochastic geometry. At last, we define the spatial capacity as our performance metric.

A. Transmission Schemes

We focus on the proposed scheme with SIR-threshold based scheduling. For comparison, we also consider a reference scheme without any transmission scheduling. For both transmission schemes, we assume that all transmitters transmit in a synchronized time-slotted manner. We also assume that all transmitters transmit at the same power level,[1] which is normalized to be unity for convenience.

1) SIR-Threshold Based Scheme: Based on the probe-and-transmit protocol, in each time slot, N probing phases with $1 \leq N < \infty$ are sequentially implemented before the data transmission phase. We assume N is a pre-given parameter and its effects will be studied later in Section IV-B. Moreover, as shown in Fig. 1, we denote the duration of a time slot and a probing phase as T and τ, respectively, with $\tau \ll T$, such that $N\tau < T$, as in [19]. By normalizing over T, the *effective data transmission time* in a time slot is obtained as $\frac{T-N\tau}{T}$, which reduces linearly over N [28]. Furthermore, we assume if a transmitter transmits probing signals in a probing phase, its intended receiver is able to measure the received signal power over the total interference power, i.e., the SIR, and feeds it back to the transmitter at the end of the probing phase. The specific algorithm design on SIR estimation and feedback is out of the scope of this paper and is not our focus. To obtain tractable analysis, we assume perfect SIR estimation and feedback in this paper, and thus the SIR value is exactly known at the transmitter; however, the impact of finite SIR estimation and feedback errors on the network capacity is important to practical design and thus will also be evaluated by simulation.

According to the feedback SIR level of its own channel, each transmitter iteratively performs the threshold-based transmission decision in each P-Phase or D-Phase, for which the details are given as follows:

- In the initial probing phase, i.e., P-Phase 0, to initialize the communication between each transmitter and receiver pair, all transmitters independently transmit probing signals to their intended receivers. Each receiver then estimates the channel amplitude and phase (for possible coherent communication in the subsequent probing and data transmission phases), and measures the received SIR of the probing signal. Each transmitter receives the feedback SIR from its intended receiver at the end of P-Phase 0.

[1]In general, each transmitters can transmit at different power levels by iteratively adjusting its transmit power based on the feedback SIR information, as in [5] or [6]. However, in this paper, we mainly focus on SIR-based transmission scheduling and thus restrict transmit power adaptation to be binary for simplicity.

- In each of the remaining probing phases from P-Phase 1 to P-Phase $N-1$, by exploiting the feedback SIR in the proceeding probing phase, each transmitter decides whether to transmit in the current probing phase with a predefined SIR threshold. Specifically, suppose a transmitter transmits in P-Phase $k-1$, $1 \leq k \leq N-1$. As shown in Fig. 1, if the feedback SIR in P-Phase $k-1$ is larger than or equal to the predefined SIR-threshold, denoted by $\gamma_k \geq 0$ for P-Phase k, the transmitter continues its transmission in P-Phase k and thus receives the feedback SIR in P-Phase k; otherwise, to improve the system throughput as well as save its energy, the transmitter decides not to transmit any more in the remaining time of this slot and will seek another transmission opportunity in the next slot, so as to let other transmitters that have higher SIR levels to re-contend the current transmission opportunity.
- In the D-Phase, similar to the SIR-threshold based scheduling from P-Phase 1 to P-Phase $N-1$, if a transmitter transmits in P-Phase $N-1$ and its feedback SIR in P-Phase $N-1$ is larger than or equal to the predefined threshold, denoted by $\gamma_N \geq 0$ for the D-Phase, the transmitter sends data to its intended receiver; otherwise, the transmitter remains silent in the rest time of this slot. The data transmission is successful if the SIR at the receiver is larger than or equal to the required SIR level, denoted by $\beta > 0$.

2) Reference Scheme: There is no transmission scheduling in the reference scheme. In each time slot, we assume all transmitters transmit data directly to their intended receivers in an independent manner. Thus, the effective data transmission time for the reference scheme is 1.[2] The data transmission is successful if the SIR at the receiver is larger than or equal to the required SIR level β as the proposed scheme. Note that by implementing an initial probing phase before the data transmission, the reference scheme can be improved to be a proposed scheme with single-stage probing.

B. Network Model

In the next, we develop the network model based on stochastic geometry. For both considered transmission schemes, we focus on single-hop communication in one particular time slot.

For both schemes, we assume that all transmitters are independently and uniformly distributed in the unbounded two-dimensional plane $\mathbb{R}^2$. We thus model the locations of all the transmitters by a homogeneous PPP with density λ. Due to the lack of central infrastructure for coordination in the wireless ad hoc network, we assume the transmitters have no knowledge about their surrounding wireless environment, and thus intend to transmit independently in a time slot with probability $\theta \in (0,1)$, as in [1]-[4]. Denote $\lambda_0 = \lambda\theta$ as the density of the initial

[2]It is worth pointing out that for the reference scheme, an initial training is needed prior to data transmission for the receiver to estimate the channel for coherent communication, similar to the initial probing of the proposed scheme with $N=1$, but without the SIR feedback to the transmitter. Here, we have assumed that such training incurs a negligible time overhead as compared to each slot duration.

transmitters that have the intention to transmit in a particular time slot. According to the Coloring theory [15], the process of the initial transmitters for both schemes is a homogeneous PPP with density λ_0, which is denoted by Φ_0. Without loss of generality, we assume λ and θ and hence λ_0 are given parameters, and will discuss the effects of λ_0 later in Section III-C. We assume each transmitter has one intended receiver, which is uniformly distributed on a circle of radius d meters (m) centered at the transmitter. We denote the locations of the i-th transmitter and its intended receiver as x_i, with $x_i \in \Phi_0$, and r_i (not included in Φ_0), respectively. The path loss between the i-th transmitter and the j-th receiver is given by $l_{ij} = |x_i - r_j|^{-\alpha}$, where $\alpha > 2$ is the path-loss exponent. We use h_{ij} to denote the distance-independent channel fading coefficient from transmitter i to receiver j. We assume flat Rayleigh fading, where all h_{ij}'s are independent and exponentially distributed random variables with unit mean. We also assume that h_{ij}'s do not change within one time-slot. We denote the SIR at the i-th receiver as $\text{SIR}_i^{(0)}$, which is given by

$$\text{SIR}_i^{(0)} = \frac{h_{ii} d^{-\alpha}}{\sum_{x_j \in \Phi_0, j \neq i} h_{ji} l_{ji}}. \tag{1}$$

Note that for the reference scheme without transmission scheduling, $\text{SIR}_i^{(0)}$ gives the received SIR level at the i-th receiver for the data transmission of transmitter i. As a result, in the reference scheme, the data transmission of transmitter i is *successful* if $\text{SIR}_i^{(0)} \geq \beta$ is satisfied.

Unlike the reference scheme, in the proposed scheme, $\text{SIR}_i^{(0)}$ only gives the received SIR level at the i-th receiver in the initial probing phase P-Phase 0. We then denote the point process formed by the retained transmitters in P-Phase k with $1 \leq k \leq N-1$, or the D-Phase with $k = N$, as Φ_k. We also denote $\text{SIR}_i^{(k)}$ as the received SIR at the i-th receiver in Φ_k. Clearly, we have $\Phi_k = \{x_i \in \Phi_{k-1} : \text{SIR}_i^{(k-1)} \geq \gamma_k\}$, where the number of transmitters in Φ_k is reduced as compared to that in Φ_{k-1}. Thus, it is easy to verify that $\text{SIR}_i^{(k)} \geq \text{SIR}_i^{(k-1)}$ for any given $\gamma_k \geq 0$, $\forall i \in \Phi_{k-1} \cap \Phi_k$. Moreover, similar to $\text{SIR}_i^{(0)}$, for any Φ_k, $k \in \{1, ..., N\}$, we can express $\text{SIR}_i^{(k)}$ as

$$\text{SIR}_i^{(k)} = \frac{h_{ii} d^{-\alpha}}{\sum_{x_j \in \Phi_k, j \neq i} h_{ji} l_{ji}}, \quad k \in \{1, ..., N\}. \tag{2}$$

It is worth noting that due to the SIR-based scheduling, the transmitters are not retained independently in Φ_k. Thus, unlike $\text{SIR}_i^{(0)}$ in (1), which is determined by the homogeneous PPP Φ_0, $\text{SIR}_i^{(k)}$ in (2) is determined by the *non-PPP* Φ_k in general [15]. For the proposed scheme, the data transmission of transmitter i is *successful* if $\text{SIR}_i^{(k-1)} \geq \gamma_k$, $\forall k \in \{1, ..., N\}$, and $\text{SIR}_i^{(N)} \geq \beta$ are all satisfied.

C. Spatial Capacity

Due to the stationarity of the homogeneous PPP Φ_0, it is easy to verify that Φ_k, $\forall k \in \{1, ...N\}$, is also stationary [4]. We thus consider a typical pair of transmitter and receiver in this paper. Without loss of generality, we assume

that the typical receiver is located at the origin. The typical pair of transmitter and receiver is named pair 0, i.e., $i = 0$. Denote the *successful transmission probability* of the typical pair in the data transmission phase of the proposed scheme with N probing phases or the reference scheme as $\mathcal{P}_0^{p,N}$ or $\mathcal{P}_0^r$, respectively. We thus have

$$\mathcal{P}_0^{p,N} = \mathbb{P}(\text{SIR}_0^{(0)} \geq \gamma_1, ..., \text{SIR}_0^{(N-1)} \geq \gamma_N, \text{SIR}_0^{(N)} \geq \beta). \tag{3}$$

$$\mathcal{P}_0^{r} = \mathbb{P}(\text{SIR}_0^{(0)} \geq \beta). \tag{4}$$

We adopt *spatial capacity* as our performance metric, which is defined as the spatial density of successful transmissions, or more specifically the average number of transmitters with successful data transmission per unit area. Considering the effective data transmission time in a time slot, we thus define the spatial capacity by the proposed scheme with N probing phases and the reference scheme as $\mathcal{C}^{p,N}$ and $\mathcal{C}^r$, respectively, given by

$$\mathcal{C}^{p,N} \triangleq \frac{T - N\tau}{T} \lambda_0 \mathcal{P}_0^{p,N}, \tag{5}$$

$$\mathcal{C}^{r} \triangleq \lambda_0 \mathcal{P}_0^{r}. \tag{6}$$

For the reference scheme, it is noted that $\mathcal{P}^r$, given in (4), is the complementary cumulative distribution function (CCDF) of $\text{SIR}_0^{(0)}$ taken at the value of β. We then have the following proposition.

Proposition 2.1: The successful transmission probability in the reference scheme is

$$\mathcal{P}_0^{r} = \exp(-\pi \lambda_0 d^2 \beta^{\frac{2}{\alpha}} \rho), \tag{7}$$

where $\rho = \int_0^\infty \frac{1}{1+v^{\alpha/2}}\, dv$. When $\alpha = 4$, we have $\rho = \frac{\pi}{2}$.

The proof of Proposition 2.1 is similar to that of [30, Theorem 2], which is based on the probability generating functional (PGFL) of the PPP, and thus is omitted here.

Since the network interference level in the D-Phase increases over the initial transmitter density λ_0, we find that $\mathcal{P}_0^r$ in (7) monotonically decreases over λ_0 as expected. Moreover, from (6) and (7), we can obtain the expression of $\mathcal{C}^r$ as

$$\mathcal{C}^{r} = \lambda_0 \exp(-\pi \lambda_0 d^2 \beta^{\frac{2}{\alpha}} \rho). \tag{8}$$

It is observed from (8) that unlike $\mathcal{P}_0^r$, the spatial capacity $\mathcal{C}^r$ does not vary monotonically over λ_0, since $\mathcal{C}^r$ can be benefited by increasing λ_0 if the resulting interference is acceptable. Moreover, from (7) and (8), it is also expected that both $\mathcal{P}_0^r$ and $\mathcal{C}^r$ monotonically decrease over the distance d between each transmitter and receiver pair, due to the reduced signal power received at the receiver, and decrease over the required SIR level β.

Unlike the reference scheme, which is determined by the homogeneous PPP Φ_0, the proposed scheme is jointly determined by Φ_0 and a sequence of non-PPPs $\{\Phi_k\}$, $1 \leq k \leq N$, where the resulting SIR distributions are

correlated. Therefore, it is very difficult to analyze/characterize the spatial capacity of the proposed scheme with N probing phases. To start up, in the next section, we focus on a simple case with single-stage probing ($N = 1$) for some insightful results.

III. SIR-Threshold based Scheme with Single-Stage Probing

In this section, we consider the proposed scheme with single-stage probing, i.e., $N = 1$. In this case, there is only one round of SIR-based scheduling, which is implemented with the threshold γ_1. For notational simplicity, for the case of $N = 1$, we omit the superscript N and use $\mathcal{P}_0^p$ and $\mathcal{C}^p$ to represent the successful transmission probability and the spatial capacity of the typical transmitter, respectively. Based on (3), the successful transmission probability for the case of $N = 1$ is reduced to

$$\mathcal{P}_0^p = \mathbb{P}(\text{SIR}_0^{(0)} \geq \gamma_1, \text{SIR}_0^{(1)} \geq \beta) \tag{9}$$

$$= \mathbb{P}(\text{SIR}_0^{(0)} \geq \gamma_1)\mathbb{P}(\text{SIR}_0^{(1)} \geq \beta | \text{SIR}_0^{(0)} \geq \gamma_1). \tag{10}$$

Moreover, when $N = 1$, the effective data transmission time for the proposed scheme is $\frac{T-\tau}{T}$. Since $\tau \ll T$, we assume the single-stage probing overhead is negligible; and thus, the effective data transmission time becomes 1 as the reference scheme. Consequently, based on (5), we can express the spatial capacity $\mathcal{C}_0^p$ as

$$\mathcal{C}^p = \lambda_0 \mathcal{P}_0^p. \tag{11}$$

Furthermore, by substituting (10) to (11), we can express $\mathcal{C}^p$ alternatively as

$$\begin{aligned}\mathcal{C}^p =& \lambda_0 \mathbb{P}(\text{SIR}_0^{(0)} \geq \gamma_1)\mathbb{P}(\text{SIR}_0^{(1)} \geq \beta | \text{SIR}_0^{(0)} \geq \gamma_1) \\ =& \lambda_1 \mathbb{P}(\text{SIR}_0^{(1)} \geq \beta | \text{SIR}_0^{(0)} \geq \gamma_1)\end{aligned} \tag{12}$$

where $\lambda_1 = \lambda_0 \mathbb{P}(\text{SIR}_0^{(0)} \geq \gamma_1)$ is the density of Φ_1 in the D-Phase, with $\lambda_1 \leq \lambda_0$. Based on Proposition 2.1, by replacing β with γ_1, it is easy to find that

$$\lambda_1 = \lambda_0 \exp\big(- \pi \lambda_0 d^2 \gamma_1^{\frac{2}{\alpha}} \rho \big). \tag{13}$$

In the following two subsections, we compare the spatial capacity of the two considered schemes, and characterize $\mathcal{C}^p$ for the proposed scheme.

A. Spatial Capacity Comparison and Closed-form Characterization with $\gamma_1 = 0$ and $\gamma_1 \geq \beta$

In this subsection, we compare the spatial capacity of the proposed scheme with that of the reference scheme. We then characterize the spatial capacity $\mathcal{C}^p$ for the proposed scheme and obtain closed-form expressions for the cases of $\gamma_1 = 0$ and $\gamma_1 \geq \beta$.

First, from (6) and (11), to compare $\mathcal{C}^p$ and $\mathcal{C}^r$, the key is to compare $\mathcal{P}_0^p$ and $\mathcal{P}_0^r$. In the reference scheme, denote the total interference power received at the typical receiver as $I_0 = \sum_{x_i \in \Phi_0, i \neq 0} h_{i0} l_{i0}$. In the proposed scheme, the received total interference power at the typical receiver in P-Phase 0 is thus I_0, while that in the D-Phase is given by $I_1 = \sum_{x_i \in \Phi_1, i \neq 0} h_{i0} l_{i0}$. For any $\gamma_1 \geq 0$, we have $I_0 \geq I_1$ since $\Phi_1 \subseteq \Phi_0$, and thus $\text{SIR}_i^{(1)} \geq \text{SIR}_i^{(0)}$. As a result, by changing over the value of $\gamma_1 \in [0, \infty)$, we obtain the following proposition.

Proposition 3.1: Given the required SIR level $\beta > 0$, for any $\gamma_1 \in [0, \infty)$, we have

$$\begin{cases} \mathcal{C}^p > \mathcal{C}^r, \text{ if } 0 < \gamma_1 < \beta \ \big(\textit{conservative} \text{ transmission regime}\big) \\ \mathcal{C}^p = \mathcal{C}^r, \text{ if } \gamma_1 = 0 \text{ or } \gamma_1 = \beta \ \big(\textit{neutral} \text{ transmission regime}\big) \\ \mathcal{C}^p < \mathcal{C}^r, \text{ if } \gamma_1 > \beta \ \big(\textit{aggressive} \text{ transmission regime}\big). \end{cases} \tag{14}$$

Proof: Please refer to Appendix A. ■

Remark 3.1: Compared to the spatial capacity of the reference scheme, Proposition 3.1 shows that for the proposed scheme with SIR-threshold based scheduling, due to the reduced interference level in the D-Phase, the spatial capacity is improved in the conservative transmission regime with $0 < \gamma_1 < \beta$. However, in the case of the aggressive transmission regime with $\gamma_1 > \beta$, where the transmitters that are able to transmit successfully in the D-Phase may also be removed from transmission, the retained transmitters in the D-Phase are *overly* reduced. Consequently, the spatial capacity is reduced in the aggressive transmission regime. It is also noted that in the neutral transmission regime with $\gamma_1 = 0$ or $\gamma_1 = \beta$, the spatial capacity is identical for the two schemes. At last, it is worth noting that Proposition 3.1 holds regardless of the specific channel fading distribution and/or transmitter location distribution.

Next, we characterize the spatial capacity $\mathcal{C}^p$ for the proposed scheme with $N = 1$. We focus on deriving the successful transmission probability $\mathcal{P}_0^p$ in (9). Unlike $\mathcal{P}_0^r$ in (4), which is given by the marginal CCDF of $\text{SIR}_0^{(0)}$ taken at value β, $\mathcal{P}_0^p$ is given by the *joint* CCDF of $\text{SIR}_0^{(0)}$ and $\text{SIR}_0^{(1)}$ taken at values (γ_1, β). In the following, we consider three cases $\gamma_1 = 0$, $\gamma_1 \geq \beta$, and $0 < \gamma_1 < \beta$, and find closed-form spatial capacity expressions for both cases of $\gamma_1 = 0$ and $\gamma_1 \geq \beta$.

Specifically, for the simple case with $\gamma_1 = 0$, we can infer from Proposition 3.1 directly that $\mathcal{C}^p = \mathcal{C}^r$, which is given in (8). For the case of $\gamma_1 \geq \beta$, since $\text{SIR}_0^{(1)} > \text{SIR}_0^{(0)}$, we have $\mathbb{P}(\text{SIR}_0^{(1)} \geq \beta | \text{SIR}_0^{(0)} \geq \gamma_1) = 1$. According to (10), we thus obtain $\mathcal{P}_0^p = \mathbb{P}(\text{SIR}_0^{(0)} \geq \gamma_1)$ in this case. By replacing β with γ_1 in Proposition 2.1, we further obtain that $\mathcal{P}_0^p = \exp(-\pi \lambda_0 d^2 \gamma_1^{\frac{2}{\alpha}} \rho)$. As a result, based on (11), we can express $\mathcal{C}^p$ for the case of $\gamma_1 \geq \beta$ as

$$\mathcal{C}^p = \lambda_0 \exp(-\pi \lambda_0 d^2 \gamma_1^{\frac{2}{\alpha}} \rho). \tag{15}$$

Similar to $\mathcal{C}^r$ given in (8), it is observed that $\mathcal{C}^p$ for both cases of $\gamma_1 = 0$ and $\gamma_1 \geq \beta$ does not vary monotonically over λ_0, but monotonically decreases over the distance d between each transmitter and receiver pair. Moreover,

unlike $\mathcal{C}^r$ and $\mathcal{C}^p$ for $\gamma_1 = 0$, $\mathcal{C}^p$ for $\gamma_1 \geq \beta$ is not related to the required SIR level β any more, since all the retained transmitters in the D-Phase meet the condition $\text{SIR}_i^{(1)} \geq \beta$ in this case.

However, for the case of $0 < \gamma_1 < \beta$, $\mathcal{P}_0^p$ cannot be simply expressed by a marginal CCDF of $\text{SIR}_0^{(0)}$ as in the above two cases. Moreover, from (9), due to the correlation between $\text{SIR}_0^{(0)}$ and $\text{SIR}_0^{(1)}$ as well as the underlying non-PPP Φ_1 that determines $\text{SIR}_0^{(1)}$, it is very difficult, if not impossible, to find an exact expression of $\mathcal{P}_0^p$ and thus $\mathcal{C}^p$ in this case. As a result, in the next subsection, we focus on finding a tight approximate to $\mathcal{C}^p$ with a tractable expression for the case of $0 < \gamma_1 < \beta$.

B. Approximate Approaches for Spatial Capacity Characterization with $0 < \gamma_1 < \beta$

This subsection focuses on approximating the spatial capacity of the proposed scheme for the case of $0 < \gamma_1 < \beta$. We first propose a new approximate approach for $\mathcal{C}^p$ and obtain an integral-based expression. Next, to find a closed-form expression for $\mathcal{C}^p$, we further approximate the integral-based expression obtained by the proposed approach. At last, we apply the conventional approximate approach in the literature and discuss its approximate performance. The details of the three approximate approaches are given as follows.

1) Proposed Approximation: From (9), to find a good approximate to $\mathcal{P}_0^p$ and thus $\mathcal{C}^p$, the key is to find a good approximate to the joint SIR distributions in Φ_0 and Φ_1. Since $\Phi_1 \subseteq \Phi_0$, we first divide the initial PPP Φ_0 into two *disjoint non-PPPs*: one is Φ_1, and the other is its complementary set $\Phi_1^c = \Phi_0 - \Phi_1$, which is the point process formed by the non-retained transmitters in the D-Phase. We denote the density of Φ_1^c as $\lambda_1^c = \lambda_0 - \lambda_1$. Clearly, Φ_1 and Φ_1^c are mutually dependent. Denote the received SIR level at the typical receiver in Φ_1^c as $\text{SIR}_0^{(1,c)} = h_{00} d^{-\alpha} / \sum_{i \in \Phi_1^c} h_{i0} l_{i0}$. Since $\Phi_1 \cup \Phi_1^c = \Phi_0$ and $\Phi_1 \cap \Phi_1^c = \emptyset$, we have $1/\text{SIR}_0^{(0)} = 1/\big(\text{SIR}_0^{(1)} + \text{SIR}_0^{(1,c)}\big)$. As a result, (9) can be equally represented by using the joint distributions of $\text{SIR}_0^{(1)}$ and $\text{SIR}_0^{(1,c)}$.

Next, we state an assumption, based on which we can use a homogeneous PPP to approximate Φ_1 and Φ_1^c, respectively, such that the existing results on PPP interference distribution in the literature can be applied to approximate the joint distributions of $\text{SIR}_0^{(1)}$ and $\text{SIR}_0^{(1,c)}$.

Assumption 1: In the proposed scheme with $N = 1$, the transmitters are retained independently in the D-Phase, with probability $\mathbb{P}(\text{SIR}_0^{(0)} \geq \gamma_1)$.

By applying Assumption 1, we denote the resulting point processes formed by the retained and non-retained transmitters in the D-Phase as $\hat{\Phi}_1$ and $\hat{\Phi}_1^c$, respectively. Clearly, both $\hat{\Phi}_1$ and $\hat{\Phi}_1^c$ are homogeneous PPPs. Moreover, the density of $\hat{\Phi}_1$ or $\hat{\Phi}_1^c$ is the same as that of Φ_1 or Φ_1^c, respectively. Since the two homogeneous PPPs $\hat{\Phi}_1$ and $\hat{\Phi}_1^c$ are disjoint, they are *independent* of each other [15]. Denote $\hat{I}_1 = \sum_{i \in \hat{\Phi}_1} h_{i0} l_{i0}$ and $\hat{I}_1^c = \sum_{i \in \hat{\Phi}_1^c} h_{i0} l_{i0}$ as the received interference power at the typical receiver in $\hat{\Phi}_1$ and $\hat{\Phi}_1^c$, respectively. We then use $f_{\hat{I}_1}(x_1)$ and $f_{\hat{I}_1^c}(x_2)$ to

denote the probability density functions (pdfs) of $\hat{I}_1$ and $\hat{I}_1^c$, respectively. The following lemma gives the general interference pdf in a homogeneous PPP-based network with Rayleigh fading channels, which is a well-known result in the literature (e.g., [31]).

Lemma 3.1: For any homogeneous PPP of density $\lambda \geq 0$, if the channel fading is Rayleigh distributed, the pdf of the received interference I at the typical receiver is given by

$$f_I(x) = \frac{1}{\pi x} \sum_{i=1}^{\infty} \frac{(-1)^{i+1} \Gamma(1+2i/\alpha) \sin(2\pi i/\alpha)}{i!} \left(\frac{\lambda \pi^2 2/\alpha}{x^{2/\alpha} \sin(2\pi/\alpha)} \right)^i. \tag{16}$$

Moreover, when $\alpha = 4$, (16) can be further expressed in a simpler closed-form as

$$f_I(x) = \frac{\lambda}{4} \left(\frac{\pi}{x} \right)^{3/2} \exp\Big(- \frac{\pi^4 \lambda^2}{16x} \Big). \tag{17}$$

As a result, based on Lemma 3.1, by substituting $\lambda = \lambda_1$ to (16) and (17), we can obtain $f_{\hat{I}_1}(x_1)$ for the cases of general α and $\alpha = 4$, respectively. Similarly, with $\lambda = \lambda_1^c$, from (16) and (17) we can obtain $f_{\hat{I}_1^c}(x_2)$ for general α and $\alpha = 4$, respectively. Therefore, by approximating Φ_1 and Φ_1^c by $\hat{\Phi}_1$ and $\hat{\Phi}_1^c$, respectively, we can easily approximate the joint distribution of $\text{SIR}_0^{(1)}$ and $\text{SIR}_0^{(1,c)}$ based on the interference pdfs $f_{\hat{I}_1}(x_1)$ and $f_{\hat{I}_1^c}(x_2)$, and thereby obtain an integral-based approximate to $\mathcal{P}_0^p$ in the following proposition.

Proposition 3.2: The successful transmission probability by the proposed scheme for the case of $0 < \gamma_1 < \beta$ is approximated as

$$\mathcal{P}_0^p \approx \int_0^{\infty} e^{-h_{00}} \int_0^{\frac{h_{00}}{\beta d^{\alpha}}} f_{\hat{I}_1}(x_1) \int_0^{\frac{h_{00}}{\gamma_1 d^{\alpha}} - x_1} f_{\hat{I}_1^c}(x_2)\, dx_2\, dx_1\, dh_{00}. \tag{18}$$

Proof: Please refer to Appendix B. ■

Finally, by multiplying λ_0 with the right-hand side of (18), we obtain an integral-based approximate to $\mathcal{C}^p$ for the case of $0 < \gamma_1 < \beta$ as

$$\mathcal{C}^p \approx \lambda_0 \int_0^{\infty} e^{-h_{00}} \int_0^{\frac{h_{00}}{\beta d^{\alpha}}} f_{\hat{I}_1}(x_1) \int_0^{\frac{h_{00}}{\gamma_1 d^{\alpha}} - x_1} f_{\hat{I}_1^c}(x_2)\, dx_2\, dx_1\, dh_{00}. \tag{19}$$

Note that the proposed approximate approach considers the correlation between $\text{SIR}_0^{(0)}$ and $\text{SIR}_0^{(1)}$, and only adopts PPP-based approximation to approximate Φ_1 and Φ_1^c by $\hat{\Phi}_1$ and $\hat{\Phi}_1^c$, respectively. Since it has been shown in the literature (e.g., [23]-[26]) that such PPP-based approximation can provide tight approximate to the corresponding non-PPP, the proposed approximate approach is able to provide tight spatial capacity approximate to $\mathcal{C}^p$ for the case of $0 < \gamma_1 < \beta$.

2) Closed-form Approximation for (19): Although the spatial capacity expression obtained in (19) is easy to integrate, it is not of closed-form. Thus, based on (18), we focus on finding a closed-form approximate to $\mathcal{P}_0^p$ and thus $\mathcal{C}^p$. We first increase the upper limit of $f_{\hat{I}_1^c}(x_2)$ in (18) from $\gamma_1 d^{\alpha} - x_1$ to $\gamma_1 d^{\alpha}$ to obtain an upper bound

for the right-hand side of (18). Then by properly lower-bounding the obtained upper bound based on Chebyshev's inequality [32], we obtain a closed-form approximate to $\mathcal{P}_0^p$, which is shown in the following proposition.

Proposition 3.3: Based on the integral-based expression given in (18), a closed-form approximate to $\mathcal{P}_0^p$ for the case of $0 < \gamma < \beta$ is obtained as

$$\mathcal{P}_0^p \approx \exp(-\pi\lambda_1 d^2 \beta^{\frac{2}{\alpha}}\rho)\exp(-\pi\lambda_1^c d^2 \gamma_1^{\frac{2}{\alpha}}\rho). \tag{20}$$

Proof: Please refer to Appendix C. ■

From (11), (13) and (20), we obtain a closed-form approximate to spatial capacity of the proposed scheme for the case of $0 < \gamma_1 < \beta$ as

$$\begin{aligned}\mathcal{C}^p \approx & \lambda_0 \times \exp\big(-\pi\lambda_0 d^2 \gamma_1^{\frac{2}{\alpha}}\rho\big) \times \exp\big[-\pi\lambda_0 \exp(-\pi\lambda_0 d^2 \gamma_1^{\frac{2}{\alpha}}\rho) d^2 \beta^{\frac{2}{\alpha}}\rho\big] \\ & \times \exp\big[\pi\lambda_0 \exp(-\pi\lambda_0 d^2 \gamma_1^{\frac{2}{\alpha}}\rho) d^2 \gamma_1^{\frac{2}{\alpha}}\rho\big].\end{aligned} \tag{21}$$

3) Conventional Approximation: It is noted that the conventional approximate approach in the literature (e.g., [23]-[26]), which only focuses on dealing with the non-PPP Φ_1, can often yield a closed-form expression. Thus, in the following, we apply the conventional approximate approach and discuss its approximate performance to $\mathcal{C}^p$.

First, since only the performance in Φ_1 is concerned by the conventional approximate approach, it takes $\mathbb{P}\big(\mathrm{SIR}_0^{(1)} \geq \beta\big)$ as the successful transmission probability of the typical transmitter in the D-Phase. Next, the non-PPP Φ_1 is approximated by the homogeneous PPP $\hat{\Phi}_1$ under Assumption 1. We denote the received SIR at the typical receiver in $\hat{\Phi}_1$ as $\mathrm{SIR}_0^{(\hat{1})} = h_{00} d^{-\alpha} / \sum_{i\in\hat{\Phi}_1} h_{i0} l_{i0}$. Thus, $\mathbb{P}\big(\mathrm{SIR}_0^{(1)} \geq \beta\big)$ is approximated by $\mathbb{P}\big(\mathrm{SIR}_0^{(\hat{1})} \geq \beta\big)$. At last, by adopting the product of λ_1 and $\mathbb{P}\big(\mathrm{SIR}_0^{(\hat{1})} \geq \beta\big)$ as an approximate to the spatial capacity $\mathcal{C}^p$, a closed-form approximate to $\mathcal{C}^p$ for the case of $0 < \gamma_1 < \beta$ is obtained as

$$\mathcal{C}^p \approx \lambda_1 \times \mathbb{P}\big(\mathrm{SIR}_0^{(\hat{1})} \geq \beta\big) \tag{22}$$

$$\overset{(a)}{=} \lambda_0 \exp\big(-\pi\lambda_0 d^2 \gamma_1^{\frac{2}{\alpha}}\rho\big) \exp\Big[-\pi\lambda_0 \exp\big(-\pi\lambda_0 d^2 \gamma_1^{\frac{2}{\alpha}}\rho\big) d^2 \beta^{\frac{2}{\alpha}}\rho\Big] \tag{23}$$

where (a) follows by Proposition 2.1 and (13). Note that since $\lambda_1 = \lambda_0 \times \mathbb{P}\big(\mathrm{SIR}_0^{(0)} \geq \gamma_1\big)$, we can rewrite (22) as $\mathcal{C}^p \approx \lambda_0 \times \mathbb{P}\big(\mathrm{SIR}_0^{(0)} \geq \gamma_1\big)\mathbb{P}\big(\mathrm{SIR}_0^{(\hat{1})} \geq \beta\big)$ under the conventional method. However, according to the definition of $\mathcal{C}^p$ for $N = 1$, which is given in (9) and (11), we have $\mathcal{C}^p = \lambda_0 \times \mathbb{P}\big(\mathrm{SIR}_0^{(0)} \geq \gamma_1, \mathrm{SIR}_0^{(1)} \geq \beta\big)$, where the distribution of $\mathrm{SIR}_0^{(1)}$ is strongly dependent on that of $\mathrm{SIR}_0^{(0)}$ as $\Phi_1 \subseteq \Phi_0$. As a result, the conventional approximate approach only focuses on the PPP-based approximate to Φ_1, but ignores the dependence between Φ_0 and Φ_1. Therefore, (22) does not hold for representing, or reasonably approximating, the spatial capacity of the proposed scheme. In addition, by comparing (21) and (23), it is observed that for the case of $0 < \gamma_1 < \beta$, given any $\lambda_0 > 0$ and

$d > 0$, the closed-form spatial capacity obtained based on the proposed approach is always outperformed that by the conventional approach.

C. Numerical Results

Numerical results are presented in this subsection. According to the method described in [15], we generate a spatial Poisson process, in which the transmitters are placed uniformly in a square of $[0\text{m}, 600\text{m}] \times [0\text{m}, 600\text{m}]$. To take care of the border effects, we focus on sampling the transmitters that locate in the interim square of $[200\text{m}, 400\text{m}] \times [200\text{m}, 400\text{m}]$. We calculate the spatial capacity as the average of the network capacity over 2000 independent network realizations, where for each network realization, the network capacity is evaluated as the ratio of the number of successful transmitters in the sampling square to the square area of $4 \times 10^2 \text{m}^2$. Unless otherwise specified, in this subsection, we set $\alpha = 4$, $\beta = 2.5$, and $d = 10\text{m}$. We also observe by simulation that similar performance can be obtained by using other parameters.

In the following, we first validate our analytical results on the spatial capacity of the proposed scheme and the reference scheme without scheduling. To highlight the spatial capacity improvement performance of the proposed scheme, we then compare the spatial capacity achieved by the propose scheme with that by two existing distributed scheduling schemes: one is the probability-based scheduling in [18], and the other is the channel-threshold based scheduling in [3] and [4]. At last, we consider a more practical scenario with SIR estimation and feedback errors, and show the effects of the SIR errors on the spatial capacity of the proposed scheme.

1) Validation of the Spatial Capacity Analysis: We validate our spatial capacity analysis in Section III-A and Section III-B for both proposed and reference schemes.

Fig. 2 shows the spatial capacity versus the SIR threshold γ_1, for both the reference scheme without transmission scheduling and the proposed scheme with SIR-based scheduling. We set the initial transmitter density as $\lambda_0 = 0.0025/\text{m}^2$ in both schemes. The analytical spatial capacity of the reference scheme is given in (8). By comparing the simulation results for the proposed scheme with the analytical results for the reference scheme, we observe that $\mathcal{C}^r$ is constant over γ_1 as expected. We also observe that 1) when $\gamma_1 < \beta$, $\mathcal{C}^p > \mathcal{C}^r$; 2) when $\gamma_1 = 0$ or $\gamma_1 = \beta$, $\mathcal{C}^p = \mathcal{C}^r$; and 3) when $\gamma_1 > \beta$, $\mathcal{C}^p < \mathcal{C}^r$. This is in accordance with our analytical results in Proposition 3.1. Moreover, for the proposed scheme, we adopt (8) and (15) as the analytical spatial capacity for the cases of $\gamma_1 = 0$ and $\gamma_1 \geq \beta$, respectively, and observe that the analytical results of the spatial capacity fit well to the simulation counterparts. Furthermore, for the case of $0 < \gamma_1 < \beta$ of the proposed scheme, where only approximate expressions for the spatial capacity are available, we compare the approximate performance of the three approximate approaches given in Section III-B. It is observed that the integral-based expression by the proposed approximate approach, given in

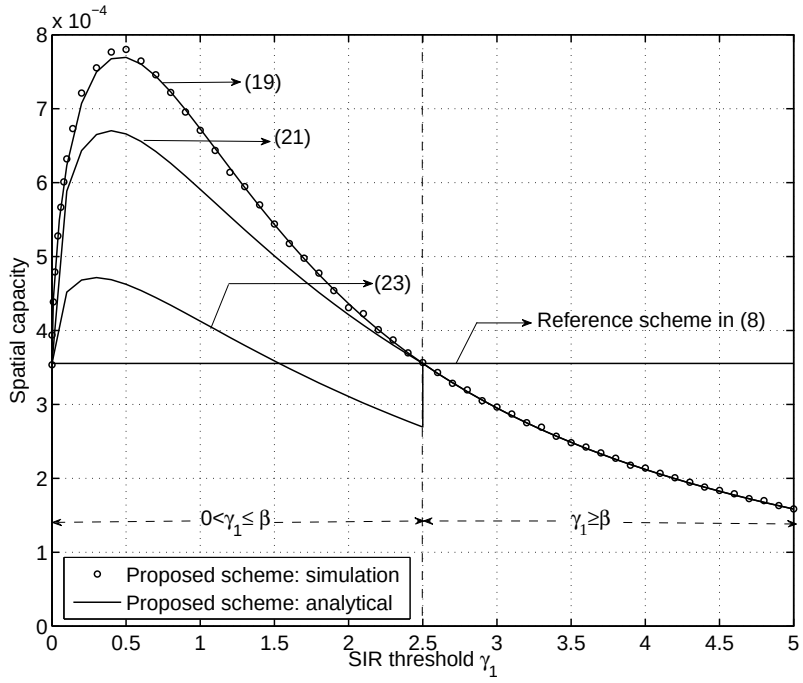

Fig. 2. Spatial capacity against γ_1 with $\lambda_0 = 0.0025$ and $\beta = 2.5$.

(19), provides a tight approximate to $\mathcal{C}^p$ for the case of $0 < \gamma_1 < \beta$. In addition, as a cost of expressing in closed-form, (21) is not as tight as (19), but (21) still provides a close approximate to $\mathcal{C}^p$ for the case of $0 < \gamma_1 < \beta$. At last, it is observed that the closed-form expression given in (23) by the conventional approximate approach cannot properly approximate $\mathcal{C}^p$ for the case of $0 < \gamma_1 < \beta$ as expected.

Fig. 3 shows the spatial capacity versus the initial transmitter density λ_0 when $\gamma_1 < \beta$. We set $\gamma_1 = 0.6$. For the proposed scheme, similar to the case in Fig. 2, we observe tight and close approximates are provided by (19) and (21), respectively, based on the proposed approximate approach, while improper approximate is provided by (23) based on the conventional approximate approach. Moreover, it is observed that the spatial capacity of the proposed scheme is always larger than that of the reference scheme, given in (8), for all values of λ_0, which is as expected from Proposition 3.1 since $\gamma_1 < \beta$ in this example. Furthermore, for both the proposed and reference schemes, we observe an interesting *density-capacity tradeoff*: by increasing λ_0, the spatial capacity first increases due to more available transmitters, but as λ_0 exceeds a certain threshold, it starts to decrease, due to the more dominant interference effect. Thus, to maximize the spatial capacity, under the system scenario set in Fig. 3, the optimal λ_0 should be set as $0.003/m^2$.

2) Performance Comparison with Existing Distributed Schemes: We consider two existing distributed scheduling schemes for performance comparison. The first scheme is the iterative probability-based scheduling as in [18].

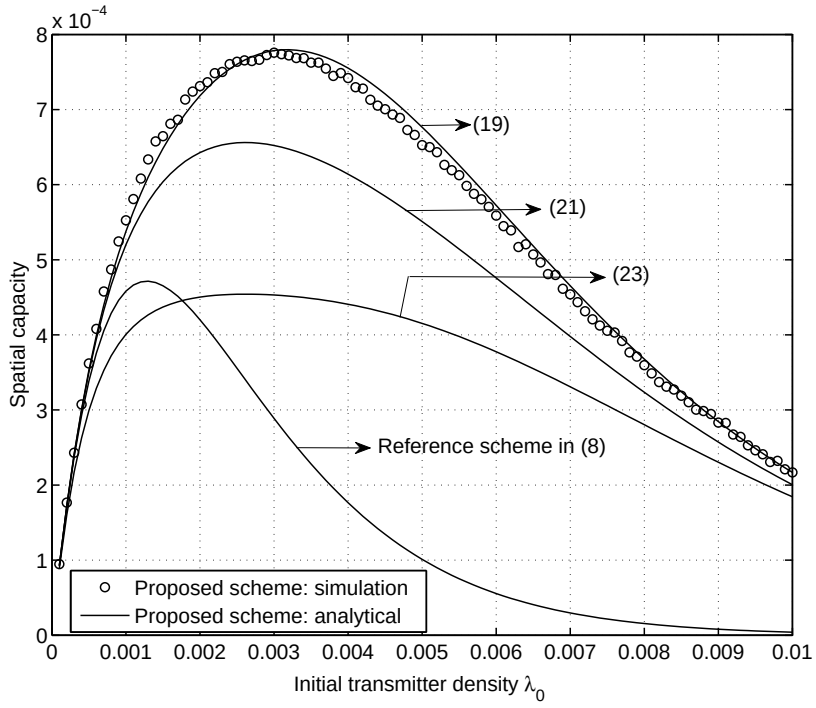

Fig. 3. Spatial capacity against λ_0. $\gamma_1 = 0.6$. $\beta = 2.5$.

Denote the transmission probability for transmitter i in P-Phase k, $1 \leq k \leq N-1$, and the D-Phase as $\phi_i^{(k)}$ or $\phi_i^{(N)}$, respectively. For any $k \in \{1, .., N\}$, [18] sets $\phi_i^{(k)} = \min\left(\frac{\text{SIR}_i^{(k-1)}}{\beta}, 1\right)$. Intuitively, [18] provides a simple and proper way to iteratively adjust the transmission probability $\phi_i^{(k)}$. The second scheme is the channel-threshold based scheduling with single-stage probing as in [3] and [4], where the received interference power is not involved in the transmission decision and each transmitter decides to transmit in the D-Phase if its direct channel strength in P-Phase 0 is no smaller than a predefined threshold γ_1', i.e., $h_{ii} \geq \gamma_1'$. For a fair comparison, we consider single-stage probing with $N = 1$ for all the proposed SIR-threshold based scheme, the probability-based scheduling in [18], and the channel-threshold based scheduling in [3] and [4].

Fig. 4 shows the spatial capacities achieved by the proposed scheme, the probability-based scheduling, the channel-threshold based scheduling, and the reference scheme without scheduling. To clearly show the effects of involving interference in the transmission decision for the proposed scheme, we set $\gamma_1' = \gamma_1 = 0.4$ for the channel-threshold based scheduling. We obtain the spatial capacity of the channel-threshold based scheduling by applying its exact expression given in [4]. Due to the lack of an exact spatial capacity expression for the probability-based scheduling, we obtain its spatial capacity by simulation. We list our observations from Fig. 4 as follows:

- *SIR based schemes v.s. channel-threshold based scheme:* It is observed that by adapting the transmission decision to the SIR, the achieved spatial capacities by both the proposed scheme and the probability-based

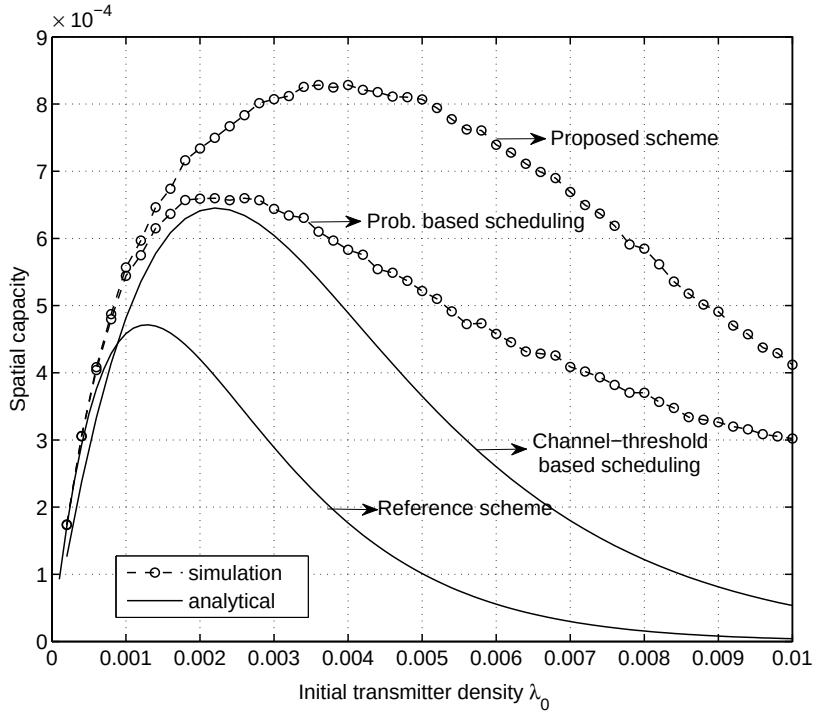

Fig. 4. Spatial capacity comparison with existing distributed scheduling schemes. $\gamma_1 = 0.4$. $\beta = 2.5$.

scheduling are always higher than that by the channel-threshold based scheduling, where the interference information is not exploited. Moreover, the spatial capacity of the channel-threshold based scheduling is smaller than that of the reference scheme when λ_0 is small, and becomes larger when λ_0 is sufficiently large. This is in sharp contrast to the cases of the proposed scheme and the probability-based scheduling, which always guarantee capacity improvement over the reference scheme without scheduling.

- *SIR-threshold based scheduling v.s. probability-based scheduling:* It is interesting to observe that although both the proposed scheme and the probability-based scheduling adapt the transmission decision to the SIR, the achieved spatial capacity by the former scheme is always higher than that by the latter one in this simulation. This is because that the proposed scheme assures the improvement of the successful transmission probability of each retained transmitter in the D-Phase, while the probability-based scheduling only assures such improvement with some probability. Moreover, it is observed that the optimal initial transmitter density that maximizes the spatial capacity of the proposed scheme is $\lambda_0^* = 0.0036$, which is larger than that for the probability-based scheduling locating at $\lambda_0^* = 0.0026$.

Note that for the proposed scheme, a lower SIR threshold γ_1 allows more transmitters to retain in the D-Phase, so as to have a second chance to transmit. Thus, by comparing the simulation results of the proposed scheme in Fig. 4 with that in Fig. 3, it is observed that the achieved optimal spatial capacity over λ_0 with $\gamma_1 = 0.4$ in Fig. 4

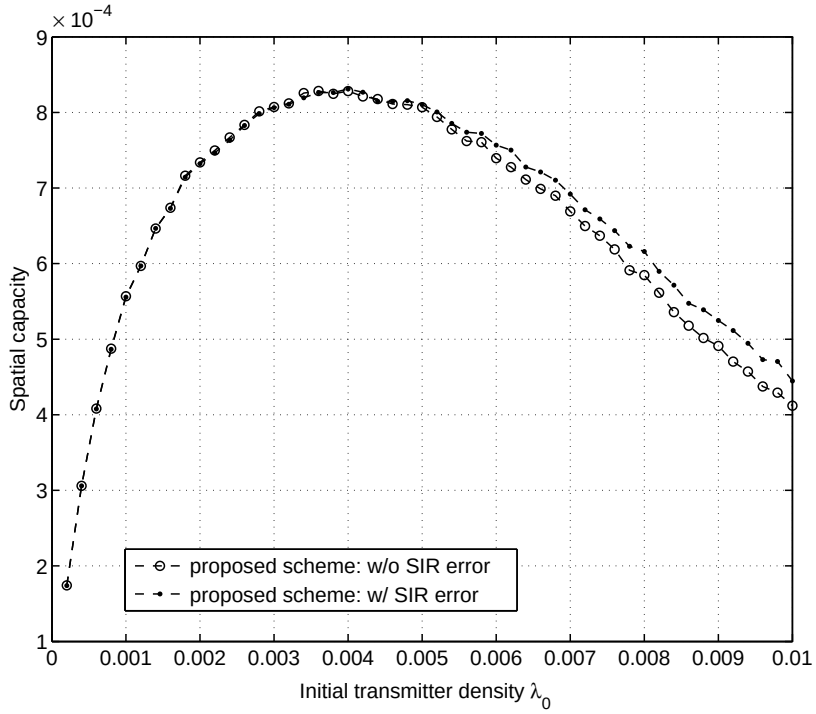

Fig. 5. Effects of the SIR errors on the spatial capacity of the proposed scheme. $\gamma_1 = 0.4$. $\beta = 2.5$.

is larger than that with $\gamma_1 = 0.6$ in Fig. 3. In addition, for all the considered schemes in Fig. 4, we observe a density-capacity tradeoff, which is similar to that in Fig. 3.

3) Effects of the SIR Estimation and Feedback Errors: We consider a more practical scenario, where SIR estimation and feedback errors exist in the implementation of the proposed scheme, and show the effects of the SIR errors on the spatial capacity. Similarly to [29], where the channel estimation and feedback errors are assumed to be zero-mean Gaussian variables, respectively, we assume the SIR estimation and feedback errors follow zero-mean Gaussian distributions with variance σ_{est}^2 and σ_{fed}^2, respectively. By further assuming that the two types of SIR errors are mutually independent, the sum of both SIR errors at transmitter i, denoted by n_i, follows zero-mean Gaussian distribution with variance $\sigma^2 = \sigma_{est}^2 + \sigma_{fed}^2$. Thus, in the presence of SIR errors, the feedback SIR level at transmitter i in P-Phase 0 is $\mathrm{SIR}_i^{(0)} + n_i$. Moreover, if the feedback SIR level $\mathrm{SIR}_i^{(0)} + n_i \geq \gamma_1$ for a given SIR threshold γ_1 in P-Phase 1, transmitter i decides to transmit in P-Phase 1; otherwise, it decides to be idle in the remaining time of this time slot. Similar to its counterpart without SIR errors in Fig. 3 and Fig. 4, the spatial capacity with SIR errors is calculated as an average value over all the transmitters' random locations, the random fading channels, as well as the random SIR errors.

Fig. 5 numerically shows the spatial capacities of the proposed scheme in both cases with and without SIR errors. We set $\sigma^2 = 10^{-2}$ and $\gamma_1 = 0.4$ in this example. It is observed from Fig. 5 that when λ_0 is small, due to

the resultant small interference in the network, each receiver i feeds back a sufficiently high SIR level $\text{SIR}_i^{(0)}$ to its associated transmitter, such that n_i has a small probability to affect the transmitter's decision. Thus, we observe that when λ_0 is small, the spatial capacity with SIR errors is tight to that without SIR errors. However, as λ_0 increases, due to the decreased $\text{SIR}_i^{(0)}$ at each transmitter i, the transmitters become more easily affected by the SIR errors n_i when deciding whether to transmit based on $\text{SIR}_i^{(0)} + n_i \geq \gamma_1$. It is noted that when λ_0 is sufficiently large, the average SIR level at each transmitter becomes very small; and even if $\text{SIR}_i^{(0)} \geq \gamma_1$ for transmitter i, $\text{SIR}_i^{(0)}$ is close to γ_1 with a large probability. Thus, under the case with zero-mean Gaussian distributed error n_i, for the transmitters with $\text{SIR}_i^{(0)} \geq \gamma_1$ in the SIR error-free case, it is more likely that these transmitters become $\text{SIR}_i^{(0)} + n_i < \gamma_1$ than $\text{SIR}_i^{(0)} + n_i \geq \gamma_1$ in the SIR error-involved case. Similarly, we can easily find that for the transmitters with $\text{SIR}_i^{(0)} < \gamma_1$ in the SIR error-free case, it is also more likely that these transmitters maintain $\text{SIR}_i^{(0)} + n_i < \gamma_1$ than $\text{SIR}_i^{(0)} + n_i \geq \gamma_1$ in the SIR error-involved case. Thus, the number of transmitters with $\text{SIR}_i^{(0)} + n_i < \gamma_1$ in the SIR error-involved case is larger than that with $\text{SIR}_i^{(0)} < \gamma_1$ in the SIR error-free case in general. Hence, as compared to the case without SIR errors, more transmitters will be refrained from transmitting in the D-Phase in the case with SIR errors, which improves the successful transmission probability in the D-Phase due to the reduced interference. As a result, it is interesting to observe from Fig. 5 that when the initial transmitter density λ_0 increases to some significant point, the spatial capacity with SIR errors becomes slightly higher than that without SIR errors; and their gap slowly increases over λ_0 after this point. Therefore, inaccurate SIR may even help improve the SIR-based scheduling performance in more interference-limited regime, which makes the proposed design robust to SIR errors.

IV. SIR-Threshold based Scheme with Multi-Stage Probing

In this section, we consider the proposed scheme with multi-stage probing, i.e., $N > 1$. In this case, N probing phases are sequentially implemented to gradually decide the transmitters that are allowed to transmit in the data transmission phase. According to (5), to find the spatial capacity $\mathcal{C}^{p,N}$ with N probing phases, we need to first find the successful transmission probability $\mathcal{P}_0^{p,N}$ given in (3). However, due to the mutually coupled user transmissions over different probing phases, the successful transmission probability in P-Phase k, $0 < k \leq N$, is related to the SIR distributions in all the proceeding probing phases (from P-Phase 0 to P-Phase $k-1$). Moreover, due to the different point process formed by the retained transmitters in each probing phase, the SIR correlations of any two probing phases are different. Thus, it is challenging to express the successful transmission probability and thus the spatial capacity for the case with $N > 1$ in general. As a result, instead of focusing on expressing the spatial capacity $\mathcal{C}^{p,N}$, we focus on studying how the key system design parameters, such as the SIR thresholds and the

number of probing phases N, affect the spatial capacity of the proposed scheme with $N > 1$. In particular, unlike the case with $N = 1$, where the single-stage overhead $N\tau = \tau \ll T$ is negligible, the multi-stage overhead $N\tau$ with $N > 1$ may not be negligible. In the following, we first study the impact of multiple SIR thresholds on the spatial capacity by extending Proposition 3.1 for the case of $N = 1$ to the case of $N > 1$. We then investigate the effects of the multi-stage probing overhead on the spatial capacity.

A. Impact of SIR Thresholds

From (3) and (5), the spatial capacity of the proposed scheme is determined by the values of SIR thresholds as well as the time overhead $N\tau$ for probing. To focus on the impact of the SIR thresholds, in this subsection, we assume $N\tau$ is negligible and thus have

$$\mathcal{C}^{p,N} = \lambda_0 \mathbb{P}\big(\mathrm{SIR}_0^{(0)} \geq \gamma_1, ..., \mathrm{SIR}_0^{(N-1)} \geq \gamma_N, \mathrm{SIR}_0^{(N)} \geq \beta\big) \tag{24}$$

where the distributions of $\mathrm{SIR}_0^{(k)}$'s, $0 \leq k \leq N$, are mutually dependent and all the Φ_k's, $1 \leq k \leq N$, are non-PPPs in general. It is also noted that for any $1 \leq k \leq N$, we have $\Phi_k \subseteq \Phi_{k-1}$ for $\gamma_k \geq 0$. Thus, the network interference level in Φ_k is reduced, as compared to that in Φ_{k-1}. As a result, by extending Proposition 3.1 for the case of $N = 1$, we obtain the following proposition for the case of $N > 1$.

Proposition 4.1: Consider two proposed schemes with arbitrary $N - 1$ and N probing phases, respectively, $N > 1$. Suppose the two schemes adopt the same SIR threshold $\gamma_k \geq 0$ in each Φ_k, $\forall k \in \{1, ..., N-1\}$. Then given $\beta > 0$, by varying the SIR threshold $\gamma_N \in [0, \infty)$ in the data transmission phase for the proposed scheme with N probing phases, we have the following relationship between $\mathcal{C}^{p,N}$ and $\mathcal{C}^{p,N-1}$ based on (24):

$$\begin{cases} \mathcal{C}^{p,N} > \mathcal{C}^{p,N-1}, \text{ if } \gamma_{N-1} < \gamma_N < \beta \ \big(\textit{conservative} \text{ transmission regime}\big) \\ \mathcal{C}^{p,N} = \mathcal{C}^{p,N-1}, \text{ if } 0 \leq \gamma_N \leq \gamma_{N-1} \text{ or } \gamma_N = \beta \ \big(\textit{neutral} \text{ transmission regime}\big) \\ \mathcal{C}^{p,N} < \mathcal{C}^{p,N-1}, \text{ if } \gamma_N > \beta \ \big(\textit{aggressive} \text{ transmission regime}\big). \end{cases} \tag{25}$$

Proof: Please refer to Appendix D. ■

Remark 4.1: Similar to the case of Proposition 3.1, in Proposition 4.1, in the conservative transmission regime with $\gamma_{N-1} < \gamma_N < \beta$, we obtain improved spatial capacity; in the aggressive transmission regime with $\gamma_N > \beta$, we obtain reduced spatial capacity; and in the neutral transmission region with $0 \leq \gamma_N \leq \gamma_{N-1}$ or $\gamma_N = \beta$, we obtain unchanged capacity. Moreover, based on the fact that the conservative transmission decision is beneficial for improving the spatial capacity of the proposed scheme, we obtain the following corollary, which gives a proper method to set the values of all the SIR-thresholds, such that the improvement of spatial capacity over the number of probing phases is assured.

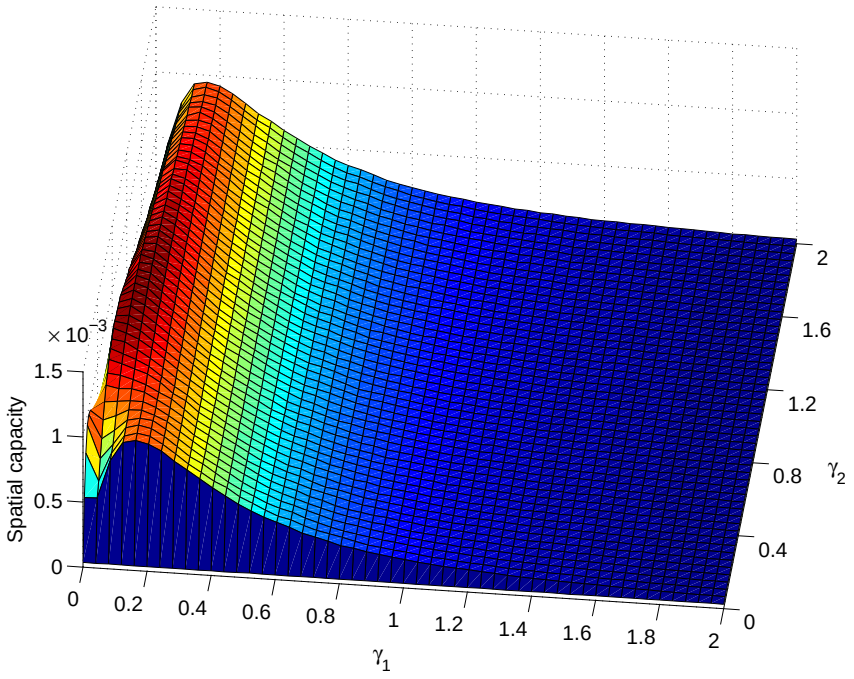

Fig. 6. Spatial capacity against γ_1 and γ_2 for $N = 2$.

Corollary 4.1: For a proposed scheme with $N>1$ probing phases with negligible overhead, if the designed SIR thresholds are properly increased as $0 < \gamma_1 < \cdots < \gamma_N < \beta$, the resulting spatial capacity $\mathcal{C}^{p,N}$ increases with the number of probing phases N.

It is worth noting that based on (24), for a given $\lambda_0 > 0$, $\mathcal{C}^{p,N}$ is only determined by the successful transmission probability $\mathcal{P}_0^{p,N}$, given in (3). Thus, both Proposition 4.1 and Corollary 4.1 also apply for $\mathcal{P}_0^{p,N}$.

In the next, we provide a numerical example with $N = 2$ to further discuss the impact of SIR thresholds on the spatial capacity. In this example, we set $\alpha = 4$, $\beta = 2$, and $d = 10$. Fig. 6 shows the corresponding spatial capacity over $\gamma_1 \in [0, \beta]$ and $\gamma_2 \in [0, \beta]$. It is observed from Fig. 6 that if $0 \leq \gamma_2 \leq \gamma_1$, the spatial capacity achieved at (γ_1, γ_2) remains unchanged over γ_2; and if $\gamma_2 > \gamma_1$, the spatial capacity achieved at (γ_1, γ_2) is always larger than that achieved at $(\gamma_1, 0)$. Apparently, this is in accordance with Proposition 4.1. Moreover, among all the points over $\gamma_1 \in [0, \beta]$ and $\gamma_2 \in [0, \beta]$, such trend is more obviously observed for small γ_1 and small γ_2. In addition, it is also observed that the spatial capacity varies much faster over γ_1 than over γ_2, and when γ_1 is sufficiently large, the resulting spatial capacity does not change much over γ_2. As a result, the SIR threshold γ_1 plays a more critical role in determining the spatial capacity than γ_2, since γ_1 determines how many transmitters can have a second chance to contend the transmission opportunity. Furthermore, it is observed that *to achieve a higher spatial capacity, it is preferred to start with a small $\gamma_1 > 0$, and then set $\gamma_2 < \beta$ with an increasing*

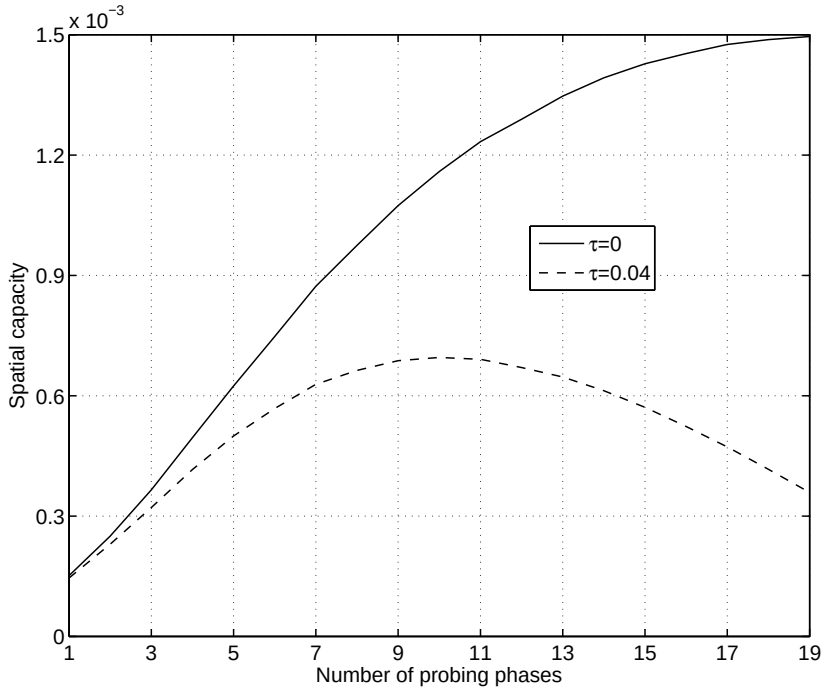

Fig. 7. Spatial capacity against the number of probing phases.

step-size, i.e., $\gamma_1 - 0 < \gamma_2 - \gamma_1$. As shown in this example, the maximum spatial capacity is achieved at $\gamma_1 = 0.15$ and $\gamma_2 = 0.8$; and the spatial capacity at $\gamma_1 = 0.15$ reduces very slowly over $\gamma_2 \in [0.8, \beta]$.

B. Effects of Multi-Stage Overhead of Probing

In this subsection, we assume the multi-stage overhead $N\tau$ for probing is not negligible and study the effects of $N\tau$ on the spatial capacity. In this case, it is easy to find from (5) that the effective data transmission time is reduced over the probing-stage number N, which reduces the spatial capacity. On the other hand, from Corollary 4.1, under the constraint that $0 < \gamma_1 < \cdots < \gamma_N < \beta$, the successful transmission probability increases over N. As a result, from (5), there exists a probing-capacity tradeoff over N under the condition that $0 < \gamma_1 < \cdots < \gamma_N < \beta$. In the following, we illustrate the probing-capacity tradeoff by a numerical example (see Fig. 7).

In this example, we show the spatial capacity of the proposed scheme over the number of probing phases N. We set $\alpha = 4$, $\beta = 2$, $d = 10$, and the time slot duration $T = 1$ second (s). We consider two cases with $\tau = 0$s and $\tau = 0.04$s, respectively, where the time overhead for probing is zero for the former case and non-negligible for the latter one. For both cases, as enlightened by Fig. 6, we start with γ_1=0.01 and gradually increase γ_k, $2 \leq k \leq N$, based on $\gamma_k = \gamma_{k-1} + 0.01k$, which gives an increasing step-size with $\gamma_k - \gamma_{k-1} < \gamma_{k+1} - \gamma_k$. To ensure $\gamma_N < \beta$, the maximum allowable N is obtained as 19. As shown in Fig. 7, it is observed that the spatial capacity increases over N for the case with $\tau = 0$, which validates Corollary 4.1. Moreover, for the case with

$\tau = 0.04$, the probing-capacity tradeoff is observed as expected: *the spatial capacity first increases over N, due to the improved performance of successful transmission probability, but after $N = 10$, the spatial capacity begins to decrease over N, due to the more dominant effects of the reduced data transmission time.*

V. Conclusion

In this paper, we addressed the spatial capacity analysis and characterization in a wireless ad hoc network by an efficient SIR-threshold based scheme. For single-stage probing, we showed the conditions under which the spatial capacity of the proposed scheme performs strictly better than that of the reference scheme without scheduling. We also characterized the spatial capacity of the proposed scheme in closed-form. In particular, we proposed a new approach to approximate the spatial capacity, which is useful for analyzing performance of wireless networks with interacted transmitters. For multi-stage probing, we extended the results for the case of single-stage probing, and gave the condition under which the spatial capacity of the proposed scheme can be gradually improved over the probing-stage number. We also studied the effects of multi-stage probing overhead and investigated the probing-capacity tradeoff.

Although the considered on/off power control in this paper is more practical than the multi-level power control for implementation [33], it is interesting to extend our network-level performance analysis to the multi-level power control in our future work. One issue needs to be properly addressed is the power convergence in the stochastic network. Unlike the power convergence studied in [5] and [6] for deterministic wireless networks, the transmit power level of each transmitter in the current probing phase is stochastically determined by the SIR distributions in all the proceeding probing phases. Moreover, due to the different point process formed by the retained transmitter in each probing phase, the SIR distributions in all the probing phases are mutually different. Although challenging, it is of our interest to find the condition that assures the power convergence in our considered stochastic network, and study the spatial capacity in a stable system with converged power level of each transmitter. In addition, we are also interested to extend our current study on synchronized transmission to the asynchronized transmission in our future work. Unlike the synchronized transmission, due to the newly added transmitters in each probing phase, it is more difficult to control and analyze the interference in each probing phase. Moreover, note that the asynchronized transmission may cause unstable communication quality for the transmitters. It is thus of our interest to design effective transmission scheme that can assure stable communication quality for all the transmitters, by effectively controlling the network interference to improve the spatial capacity in our future work.

APPENDIX A
PROOF OF PROPOSITION3.1

By expressing $\text{SIR}_0^{(0)} = h_{00}d^{-\alpha}/I_0$ and $\text{SIR}_0^{(1)} = h_{00}d^{-\alpha}/I_1$, based on (4), (6), (10) and (11), we have

$$\frac{\mathcal{C}^p}{\mathcal{C}^r} = \frac{\mathbb{P}(h_{00} \geq \gamma_1 d^\alpha I_0) \times \mathbb{P}(h_{00} \geq \beta d^\alpha I_1 | h_{00} \geq \gamma_1 d^\alpha I_0)}{\mathbb{P}(h_{00} \geq \beta d^\alpha I_0)}. \tag{26}$$

In the following, we compare $\frac{\mathcal{C}^p}{\mathcal{C}^r}$ with 1 by varying $\gamma_1 \in [0, \infty)$. Clearly, when $\gamma_1 = 0$, $\frac{\mathcal{C}^p}{\mathcal{C}^r} = 1$. Next, we consider the case of $\gamma_1 \geq \beta$. Since $I_0 \geq I_1$, if $\gamma_1 \geq \beta$, we obtain $\mathbb{P}(h_{00} \geq \beta d^\alpha I_1 | h_{00} \geq \gamma_1 d^\alpha I_0) = 1$. Moreover, for the non-negative and continuous random variables h_{00} and I_0, it is easy to find that if $\gamma_1 > \beta$, $\mathbb{P}(h_{00} \geq \gamma_1 d^\alpha I_0) < \mathbb{P}(h_{00} \geq \beta d^\alpha I_0)$, and if $\gamma_1 = \beta$, $\mathbb{P}(h_{00} \geq \gamma_1 d^\alpha I_0) = \mathbb{P}(h_{00} \geq \beta d^\alpha I_0)$. As a result, from (26), if $\gamma_1 > \beta$, $\frac{\mathcal{C}^p}{\mathcal{C}^r} < 1$, and if $\gamma_1 = \beta$, $\frac{\mathcal{C}^p}{\mathcal{C}^r} = 1$. At last, we consider the case of $0 < \gamma_1 < \beta$. In this case, we have $\mathbb{P}(h_{00} \geq \gamma_1 d^\alpha I_0 | h_{00} \geq \beta d^\alpha I_0) = 1$, or equivalently,

$$\frac{\mathbb{P}(h_{00} \geq \gamma_1 d^\alpha I_0) \times \mathbb{P}(h_{00} \geq \beta d^\alpha I_0 | h_{00} \geq \gamma_1 d^\alpha I_0)}{\mathbb{P}(h_{00} \geq \beta d^\alpha I_0)} = 1. \tag{27}$$

Moreover, since $\gamma_1 \neq 0$ in this case, we have $F_{I_1}(x) > F_{I_0}(x)$, $\forall x > 0$, where $F_{I_0}(\cdot)$ and $F_{I_1}(\cdot)$ denote the cumulative distribution functions (CDFs) of I_0 and I_1, respectively. It is then easy to verify that $\mathbb{P}(h_{00} \geq \beta d^\alpha I_1 | h_{00} \geq \gamma_1 d^\alpha I_0) > \mathbb{P}(h_{00} \geq \beta d^\alpha I_0 | h_{00} \geq \gamma_1 d^\alpha I_0)$, for which, by multiplying $\frac{\mathbb{P}(h_{00} \geq \gamma_1 d^\alpha I_0)}{\mathbb{P}(h_{00} \geq \beta d^\alpha I_0)}$ on both sides and based on (27), we have

$$\frac{\mathbb{P}(h_{00} \geq \gamma_1 d^\alpha I_0) \times \mathbb{P}(h_{00} \geq \beta d^\alpha I_1 | h_{00} \geq \gamma_1 d^\alpha I_0)}{\mathbb{P}(h_{00} \geq \beta d^\alpha I_0)} > 1.$$

That is, $\frac{\mathcal{C}^p}{\mathcal{C}^r} > 1$. Proposition 3.1 thus follows.

APPENDIX B
PROOF OF PROPOSITION 3.2

Under Assumption 1, we obtain two independent PPPs $\hat{\Phi}_1$ and $\hat{\Phi}_1^c$, with $\hat{\Phi}_1 \cup \hat{\Phi}_1^c = \Phi_0$ and $\hat{\Phi}_1 \cap \hat{\Phi}_1^c = \emptyset$. Since from (9), it follows that

$$\begin{aligned}\mathcal{P}_0^p =& \mathbb{P}(\text{SIR}_0^{(0)} \geq \gamma_1, \text{SIR}_0^{(1)} \geq \beta) \\ =& \mathbb{P}\Big(\sum_{i \in \Phi_0, i \neq 0} h_{i0} l_{i0} \leq \frac{h_{00}}{\gamma_1 d^\alpha}, \sum_{i \in \Phi_1, i \neq 0} h_{i0} l_{i0} \leq \frac{h_{00}}{\beta d^\alpha} \Big),\end{aligned}$$

we have

$$\begin{aligned}\mathcal{P}_0^p \approx& \mathbb{P}\Big(\Big(\sum_{i \in \hat{\Phi}_1, i \neq 0} h_{i0} l_{i0} + \sum_{i \in \Phi, \hat{i} \neq 0_1^c} h_{i0} l_{i0} \Big) \leq \frac{h_{00}}{\gamma_1 d^\alpha}, \sum_{i \in \hat{\Phi}_1} h_{i0} l_{i0} \leq \frac{h_{00}}{\beta d^\alpha} \Big) \\ =& \mathbb{P}\Big(\hat{I}_1 + \hat{I}_1^c \leq \frac{h_{00}}{\gamma_1 d^\alpha}, \hat{I}_1 \leq \frac{h_{00}}{\beta d^\alpha} \Big).\end{aligned}$$

Due to the independence of $\hat{\Phi}_1$ and $\hat{\Phi}_1^c$, $\hat{I}_1$ is independent of $\hat{I}_1^c$. Given h_{00}, we thus have

$$\begin{aligned}&\mathbb{P}\Big(\hat{I}_1+\hat{I}_1^c\le\frac{h_{00}}{\gamma_1 d^\alpha},\hat{I}_1\le\frac{h_{00}}{\beta d^\alpha}\Big|h_{00}\Big)\\&=\int_0^{\frac{h_{00}}{\beta d^\alpha}}f_{\hat{I}_1}(x_1)\int_0^{\frac{h_{00}}{\gamma_1 d^\alpha}-x_1}f_{\hat{I}_1^c}(x_2)\,dx_2\,dx_1.\end{aligned}\tag{28}$$

By integrating (28) over the (exponential) distribution of h_{00}, we obtain (18). Proposition 3.2 thus follows.

APPENDIX C
PROOF TO PROPOSITION 3.3

In this proof, we first derive an upper bound for the right-hand side of (18), and then by properly lower-bounding the obtained upper bound, we give a tractable approximate to $\mathcal{P}_0^p$.

First, in (18), by increasing the upper limit of $f_{\hat{I}_1^c}(x_2)$, i.e., $\gamma_1 d^\alpha - x_1$, to $\gamma_1 d^\alpha$, the tight approximation of $\mathcal{P}_0^p$ is upper-bounded as

$$\begin{aligned}\mathcal{P}_0^p&\approx\int_0^\infty e^{-h_{00}}\int_0^{\frac{h_{00}}{\beta d^\alpha}}f_{\hat{I}_1}(x_1)\int_0^{\frac{h_{00}}{\gamma_1 d^\alpha}-x_1}f_{\hat{I}_1^c}(x_2)\,dx_2\,dx_1\,dh_{00}\\&<\int_0^\infty e^{-h_{00}}\int_0^{\frac{h_{00}}{\beta d^\alpha}}f_{\hat{I}_1}(x_1)\int_0^{\frac{h_{00}}{\gamma_1 d^\alpha}}f_{\hat{I}_1^c}(x_2)\,dx_2\,dx_1\,dh_{00}.\end{aligned}\tag{29}$$

Next, denote $Y_1(h_{00})=\int_0^{\frac{h_{00}}{\beta d^\alpha}}f_{\hat{I}_1}(x_1)\,dx_1$ and $Y_2(h_{00})=\int_0^{\frac{h_{00}}{\gamma_1 d^\alpha}}f_{\hat{I}_1^c}(x_2)\,dx_2$. We can rewrite (29) as

$$\int_0^\infty e^{-h_{00}}\int_0^{\frac{h_{00}}{\beta d^\alpha}}f_{\hat{I}_1}(x_1)\int_0^{\frac{h_{00}}{\gamma_1 d^\alpha}}f_{\hat{I}_1^c}(x_2)\,dx_2\,dx_1\,dh_{00}=\mathbb{E}\big[Y_1(h_{00})Y_2(h_{00})\big].\tag{30}$$

Note that both $Y_1(h_{00})$ and $Y_2(h_{00})$ are monotonically increasing over h_{00}. Thus, according to the Chebyshev's inequality [32], the right-hand side of (30) can be lower-bounded as

$$\mathbb{E}\big[Y_1(h_{00})Y_2(h_{00})\big]\ge\mathbb{E}\big[Y_1(h_{00})\big]\mathbb{E}\big[Y_2(h_{00})\big].\tag{31}$$

For $\mathbb{E}\big[Y_1(h_{00})\big]$ in (31), by integrating $Y_1(h_{00})$ over the exponential distributed h_{00}, we obtain that

$$\begin{aligned}\mathbb{E}\big[Y_1(h_{00})\big]&=\int_0^\infty e^{-h_{00}}\int_0^{\frac{h_{00}}{\beta d^\alpha}}f_{\hat{I}_1}(x_1)\,dx_1\,dh_{00}\\&=P\Big(0\le\hat{I}_1\le\frac{h_{00}}{\beta d^\alpha}\Big)\\&\overset{(a)}{=}\exp(-\pi\lambda_1 d^2\beta^{\frac{2}{\alpha}}\rho),\end{aligned}\tag{32}$$

where (a) is obtained based on Proposition 2.1, by replacing λ_0 with λ_1. Similarly, we can obtain that

$$\mathbb{E}\big[Y_2(h_{00})\big]=\exp(-\pi\lambda_1^c d^2\gamma_1^{\frac{2}{\alpha}}\rho).\tag{33}$$

Finally, by substituting (32) and (33) into the right-hand side of (31) and then adopting the resulting right-hand side of (31) to approximate $\mathcal{P}_0^p$, we can obtain a tractable approximate to $\mathcal{P}_0^p$ for the case of $0<\gamma_1<\beta$ as in (20). Proposition 3.3 is thus proved.

APPENDIX D
PROOF TO PROPOSITION 4.1

From (24), we have

$$\mathcal{C}^{p,N} = \lambda_0 \mathbb{P}\big(\mathrm{SIR}_0^{(0)} \geq \gamma_1, ..., \mathrm{SIR}_0^{(N-1)} \geq \gamma_N\big)\mathbb{P}\big(\mathrm{SIR}_0^{(N)} \geq \beta \big| \mathrm{SIR}_0^{(0)} \geq \gamma_1, ..., \mathrm{SIR}_0^{(N-1)} \geq \gamma_N\big). \tag{34}$$

Thus, based on (24) and (34), we have

$$\frac{\mathcal{C}_0^{p,N}}{\mathcal{C}_0^{p,N-1}} = \frac{\mathbb{P}\big(\mathrm{SIR}_0^{(0)} \geq \gamma_1, \cdots, \mathrm{SIR}_0^{(N-1)} \geq \gamma_N\big)}{\mathbb{P}\big(\mathrm{SIR}_0^{(0)} \geq \gamma_1, \cdots, \mathrm{SIR}_0^{(N-1)} \geq \beta\big)}\mathbb{P}\big(\mathrm{SIR}_0^{(N)} \geq \beta \big| \mathrm{SIR}_0^{(0)} \geq \gamma_1, \cdots, \mathrm{SIR}_0^{(N-1)} \geq \gamma_N\big). \tag{35}$$

Since both proposed schemes adopt the same SIR thresholds γ_k for any $k \in \{1, ..., N-1\}$, the distributions of these $\mathrm{SIR}_0^{(k)}$'s are the same for both proposed schemes and thus do not affect the ratio of $\frac{\mathcal{C}_0^{p,N}}{\mathcal{C}_0^{p,N-1}}$. Hence, in the following, we focus on the distribution $\mathrm{SIR}_0^{(N)}$ by varying $\gamma_N \in [0, \infty)$, and compare $\frac{\mathcal{C}_0^{p,N}}{\mathcal{C}_0^{p,N-1}}$ with 1. With a proof similar to that of Proposition 3.1, it is easy to verify that

1) if $0 \leq \gamma_N \leq \gamma_{N-1}$, the distribution of $\mathrm{SIR}_0^{(N)}$ is the same as that of $\mathrm{SIR}_0^{(N-1)}$; and thus we have $\frac{\mathcal{C}_0^{p,N}}{\mathcal{C}_0^{p,N-1}} = 1$;
2) if $\gamma_N \geq \beta$, $\mathbb{P}\big(\mathrm{SIR}_0^{(N)} \geq \beta \big| \mathrm{SIR}_0^{(0)} \geq \gamma_1, \cdots, \mathrm{SIR}_0^{(N-1)} \geq \gamma_N\big) = 1$, and $\mathbb{P}\big(\mathrm{SIR}_0^{(0)} \geq \gamma_1, \cdots, \mathrm{SIR}_0^{(N-1)} \geq \gamma_N\big) \leq \mathbb{P}\big(\mathrm{SIR}_0^{(0)} \geq \gamma_1, \cdots, \mathrm{SIR}_0^{(N)} \geq \beta\big)$, where "=" holds when $\gamma_N = \beta$. Thus, from (35), if $\gamma_N > \beta$, $\frac{\mathcal{C}_0^{p,N}}{\mathcal{C}_0^{p,N-1}} < 1$, and if $\gamma_N = \beta$, $\frac{\mathcal{C}_0^{p,N}}{\mathcal{C}_0^{p,N-1}} = 1$;
3) if $\gamma_{N-1} < \gamma_N < \beta$, we have

$$\begin{aligned}\frac{\mathcal{C}_0^{p,N}}{\mathcal{C}_0^{p,N-1}} > &\frac{\mathbb{P}\big(\mathrm{SIR}_0^{(0)} \geq \gamma_1, \cdots, \mathrm{SIR}_0^{(N-1)} \geq \gamma_N\big)}{\mathbb{P}\big(\mathrm{SIR}_0^{(0)} \geq \gamma_1, \cdots, \mathrm{SIR}_0^{(N-1)} \geq \beta\big)} \\ &\times \mathbb{P}\big(\mathrm{SIR}_0^{(N-1)} \geq \beta \big| \mathrm{SIR}_0^{(0)} \geq \gamma_1, \cdots, \mathrm{SIR}_0^{(N-1)} \geq \gamma_N\big) = 1.\end{aligned}$$

Proposition 4.1 thus follows.

REFERENCES

[1] S. Weber, J. G. Andrews, and N. Jindal, "An overview of the transmission capacity of wireless networks," *IEEE Trans. Commun.*, vol. 58, no. 12, pp. 3593-3604, Dec. 2010.

[2] N. Jindal, S. Weber, and J. G. Andrews, "Fractional power control for decentralized wireless networks," *IEEE Trans. Wireless Commun.*, vol. 7, no. 12, pp. 5482-5492, Dec. 2008.

[3] S. Weber, J. G. Andrews, and N. Jindal, "The effect of fading, channel inversion and threshold scheduling on ad hoc networks," *IEEE Trans. Inf. Theory*, vol. 53, no. 11, pp. 4127-4149, Nov. 2007.

[4] F. Baccelli, B. Blaszczyszyn, and P. Muhlethaler, "Stochastic analysis of spatial and opportunistic Aloha," *IEEE J. Sel. Areas Commun.*, pp. 1105-1119, Sep. 2009.

[5] G. J. Foschini and Z. Miljanic, "A simple distributed autonomous power control algorithm and its convergence," *IEEE Trans. Veh. Technol.*, vol. 42, pp. 641646, Nov. 1993.

[6] R. D. Yates, "A framework for uplink power control in cellular radio systems," *IEEE J. Select Areas Commun.*, vol. 13, no. 7, pp. 1341-1347, Sep. 1995.

[7] T. ElBatt and A. Ephremides, "Joint scheduling and power control for wireless ad hoc networks," *IEEE Trans. Wireless Commun.*, vol. 3, no. 1, pp. 74-85, Jan. 2004.

[8] W. L. Huang and K. Letaief, "Cross-layer scheduling and power control combined with adaptive modulation for wireless ad hoc networks," *IEEE Trans. Commun.*, vol. 5, no. 4, pp. 728-739, Apr. 2007.

[9] F. Baccelli and C. Singh, "Adaptive spatial aloha, fairness and stochastic geometry." in *Proc. IEEE Int. Symp. Modeling & Optimization in Mobile, Ad Hoc & Wireless Networks (WiOpt)*, May 2013.

[10] P. Gupta and P. R. Kumar, "The capacity of wireless networks," *IEEE Trans. Inform. Theory*, vol. 46, pp. 388-404, Mar. 2000.

[11] M. Andrews and M. Dinitz, "Maximizing capacity in arbitrary wireless networks in the sinr model: complexity and game theory," in *Proc. IEEE Int. Conf. Computer Commun. (INFOCOM)*, Apr. 2009.

[12] M. Dinitz, "Distributed algorithms for approximating wireless network capacity," in *Proc. IEEE Int. Conf. Computer Commun. (INFOCOM)*, Mar. 2010.

[13] E. I. Asgeirsson and P. Mitra, "On a game theoretic approach to capacity maximization in wireless networks," in *Proc. IEEE Int. Conf. Computer Commun. (INFOCOM)*, Apr. 2011.

[14] J. G. Andrews, R. K. Ganti, N. Jindal, M. Haenggi, and S. Weber, "A primer on spatial modeling and analysis in wireless networks," *IEEE Commun. Mag.*, vol. 48, no. 11, pp. 156-163, Nov. 2010.

[15] D. Stoyan, W. S. Kendall, and J. Mecke, *Stochastic geometry and its applications*, 2nd edition. John Wiley and Sons, 1995.

[16] A. Ghosh *et al.*, "Heterogeneous cellular networks: From theory to practice," *IEEE Commun. Mag.*, vol. 50, no. 6, pp. 54-64, Jun. 2012.

[17] J. Kingman, *Poisson Processes*. Oxford University Press, USA, 1993.

[18] D. M. Kim and S. Kim, "Exploiting regional differences: A spatially adaptive random access." Available [online] at http://arxiv.org/abs/1403.3891.

[19] P. S. C. Thejaswi, J. Zhang, M.-O. Pun, H. V. Poor, and D. Zheng, "Distributed opportunistic scheduling with two-level probing," *IEEE/ACM Trans. Net.*, vol. 15, no. 5, pp. 1464-1477, Oct. 2010.

[20] F. Baccelli, B. Blaszczyszyn, and P. Mühlethaler, "An ALOHA protocol for multihop mobile wireless networks," *IEEE Trans. Inform. Theory*, vol. 52, no. 2, pp. 421-436, Feb. 2006.

[21] D. Tse and S. Hanly, "Multiaccess fading channelsPart I: Polymatroid structure, optimal resource allocation and throughput capacities," *IEEE Trans. Inform. Theory*, vol. 44, no. 7, pp. 2796-2815, Nov. 1998.

[22] S. Hanly and D. Tse, "Multiaccess fading channelsPart II: Delay-limited capacities," *IEEE Trans. Inform. Theory*, vol. 44, no. 7, pp. 2816-2831, Nov. 1998.

[23] A. Hasan and J. G. Andrews, "The guard zone in wireless ad hoc networks," *IEEE Trans. Wireless Commun.*, vol. 6, pp. 897-906, Mar. 2007.

[24] T. D. Novlan, H. S. Dhillon, and J. G. Andrews, "Analytical modeling of uplink cellular networks," *IEEE Trans. Wireless Commun.*, vol. 12, no. 6, pp. 2669-2679, Jun. 2013.

[25] H. Q. Nguyen, F. Baccell, and D. Kofman, "A stochastic geometry analysis of dense IEEE 802.11 networks," in *Proc. IEEE Int. Conf. Computer Commun. (INFOCOM)*, 2007.

[26] T. V. Nguyen and F. Baccelli, "A stochastic geometry model for cognitive radio networks," *The Computer Journal*, vol. 55, pp. 534-552, Jul. 2011.

[27] X. Song, C. Yin, D. Liu, and R. Zhang, "Spatial throughput characterization in cognitive radio networks with threshold-based opportunistic spectrum access," *IEEE J. Sel. Areas in Comm.*, to appear.

[28] E. Hossain, L. Le, N. Devroye, and M. Vu, "*Cognitive radio: from theory to practical network engineering*," *in New directions in wireless communications research.* Springer, 2009, ch. 10, pp. 251-289.

[29] H. Su and E. Geraniotis, "Adaptive closed-loop power control with quantized feedback and loop filtering," *IEEE Trans. Wireless Commun.*, vol. 1, no. 1, pp. 76-86, Jan. 2002.

[30] J. G. Andrews, F. Baccelli, and R. K. Ganti, "A tractable approach to coverage and rate in cellular networks," *IEEE Trans. Commun.*, vol. 59, no. 11, pp. 3122-3134, Nov. 2011.

[31] M. Haenggi and R. K. Ganti, *Inteference in large wireless networks.* NOW: Foundations and Trends in Networking, 2008.

[32] C. P. Niculescu and J. Pečarić, "The equivalence of Chebyshev's inequality with the Hermite-Hadamard inequality," *Math. Reports*, vol. 12(62), no. 2, pp. 145-156, 2010.

[33] J. Chamberland and V. V. Veeravalli, "Decentralized dynamic power control for cellular CDMA Systems," *IEEE Trans. Wireless Commun.*, vol. 2, no. 3, pp. 549-559, May. 2003.